

Composite of Colloidal Crystals of Silica in Poly(methyl methacrylate)

Hari Babu Sunkara, Jagdish M. Jethmalani, and Warren T. Ford*

Department of Chemistry, Oklahoma State University
Stillwater, Oklahoma 74078

Received December 16, 1993

Revised Manuscript Received February 22, 1994

Introduction

Colloidal crystals form spontaneously in both aqueous and nonaqueous dispersions of monodisperse colloidal particles.¹ The dispersions Bragg diffract visible light at specific wavelengths corresponding with the lattice spacings. They have potential applications as optical rejection filters and optical limiters. Narrow-bandwidth filters composed of monodisperse polystyrene latexes in water have been used to reject the Rayleigh scattering in a Raman spectrometer.^{2,3} The colloidal crystals of latexes orient with d_{hkl} planes parallel to the plane of the quartz cell. A major drawback with these filters is that weak shear, gravitational, electrical, and thermal forces disturb the order, due to the low elastic modulus of the liquid dispersions of colloidal crystals.^{1,4-6} We report here a solution to the stability problem. Colloidal crystals of monodisperse silica in a liquid methyl methacrylate can be polymerized to form a rigid PMMA film that retains the crystal structure. These more robust films may have wider use as selective filters and other optical devices.

Experimental Methods

Colloidal dispersions of silica in aqueous ammoniacal ethanol were prepared by the Stöber method.^{7,8} 3-(Trimethoxysilyl)-propyl methacrylate (TPM) was grafted to the silica particles by the procedure of Philipse and Vrij.⁹ The average particle diameter was measured to be 152 nm, with a polydispersity (standard deviation/mean) of 0.04, by TEM and 159 nm by dynamic light scattering. The dispersion of TPM silica in ethanol was transferred to methanol and then to methyl methacrylate by dialysis.¹⁰ We observed iridescence from the MMA dispersion but not from the methanol dispersion.

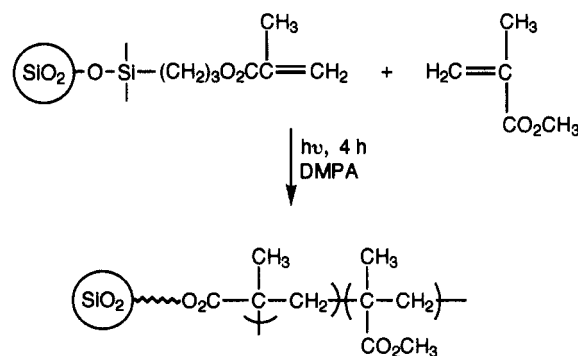
The dispersions were polymerized in glass sandwich cells made from 1 in. × 3 in. × 1 mm microscope slides with 264- μ m Teflon spacers. The cell containing the colloidal silica dispersion and the initiator, 2,2-dimethoxy-2-phenylacetophenone (DMPA, 1 wt % of monomer), was polymerized at ambient temperature for 4-5 h using a medium-pressure 450-W mercury vapor lamp 2 cm from the sample with the film plane horizontal. Spectrophotometric measurements were made with the films still in the glass cell, and the films were removed for optical and electron microscopy.

Results and Discussion

Diffraction from colloidal crystals of monodisperse charged polystyrene particles in aqueous medium has been

- (1) Okubo, T. *Prog. Polym. Sci.* **1993**, *18*, 481.
- (2) Flaugh, P. L.; O'Donnell, S. E.; Asher, S. A. *Appl. Spectrosc.* **1984**, *38*, 847.
- (3) Asher, S. A.; Flaugh, P. L.; Washinger, G. *Spectroscopy* **1986**, *1*, 26.
- (4) Clark, N. A.; Hurd, A. J.; Ackerson, B. J. *Nature* **1979**, *281*, 57.
- (5) Carlson, R. J.; Asher, S. A. *Appl. Spectrosc.* **1984**, *38*, 297.
- (6) Okubo, T. *Colloid Polym. Sci.* **1993**, *271*, 873.
- (7) Stöber, W.; Fink, A.; Bohn, E. *J. Colloid Interface Sci.* **1968**, *26*, 62.
- (8) Badley, R. D.; Ford, W. T.; McEnroe, F. J.; Assink, R. A. *Langmuir* **1990**, *6*, 792.
- (9) Philipse, A. P.; Vrij, A. *J. Colloid Interface Sci.* **1989**, *128*, 121.
- (10) Hiltner, P. A.; Papir, Y. S.; Krieger, I. M. *J. Phys. Chem.* **1971**, *75*, 1881.

Scheme 1



explained by dynamical diffraction theory which accounts interference between incident and diffracted beams:^{11,12}

$$\lambda_{\text{corr}} = \lambda \left(1 - \frac{\psi_0}{2 \sin^2 \theta} \right) \quad (1)$$

where

$$\lambda = 2n_s d_{hkl} \sin \theta \quad \psi_0 = 3\phi \frac{(m^2 - 1)}{(m^2 + 2)}$$

ψ_0 is the real part of the crystal polarizability, λ is the Bragg diffracted wavelength, d_{hkl} is the interplanar spacing, θ is the Bragg angle, m is the ratio of the refractive index of the particles to that of surrounding medium, ϕ is the particle volume fraction, and n_s is the refractive index of the suspension calculated by¹²

$$n_s = n_m(1 - \phi) + n_p \phi \quad (2)$$

n_m and n_p are the refractive indexes of the medium and particles. We have used these equations to calculate the crystal parameters in this study. According to the equations the Bragg diffraction wavelength (λ_{corr}) depends on the crystal volume fraction and the difference between the refractive indexes of the particles and the medium.

Colloidal Crystals in MMA. The chemical structure of the TPM silica particles is shown in Scheme 1. The 152-nm diameter TPM silica particles at concentrations of 35-40 wt % (19.5-22.7 vol % based on our measured density of TPM silica of 1.795 g cm⁻³) in MMA spontaneously form colloidal crystals. The structures of colloidal crystals of both polystyrene latexes in water^{1,4,12,13} and silica spheres in ethanol/toluene mixtures¹⁴ are bcc or fcc. At high volume fraction only fcc has been observed. Since silica has a much lower charge density than most polystyrene latexes and the particle concentration is high, a fcc structure is most likely for the MMA dispersions.

By orthoscopic microscopy between crossed polarizers we see during crystal growth a mosaic of 100-500- μ m crystalline domains of various colors.^{11,13} Crystal growth is faster at the edges, where the dispersion is in contact with the cured epoxy used to seal the cell, than in the center. The crystallites at the edges are blue and green, pillar shaped, and larger than the crystallites in the center. Over 4-7 days at 25 °C with the film plane horizontal, the

- (11) Monovoukas, Y.; Gast, A. P. *Langmuir* **1991**, *7*, 460.
- (12) Rundquist, P. A.; Photinos, P.; Jagannathan, S.; Asher, S. A. *J. Chem. Phys.* **1989**, *91*, 4932.
- (13) Monovoukas, Y.; Gast, A. P. *Phase Transitions* **1990**, *21*, 183.
- (14) Dhont, J. K. G.; Smits, C.; Lekkerkerker, H. N. W. *J. Colloid Interface Sci.* **1992**, *152*, 386.

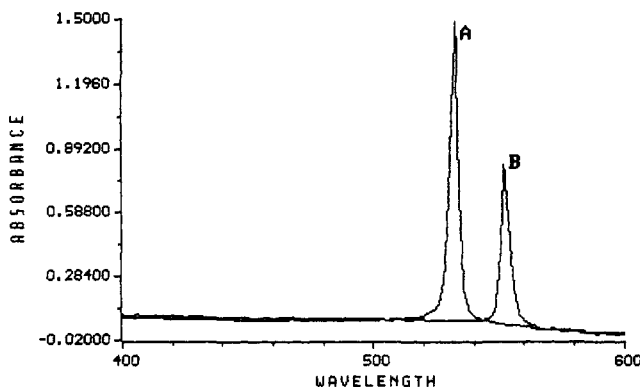


Figure 1. Visible spectra due to Bragg diffraction of 152-nm TPM silica dispersions in MMA: (A) $\phi = 0.227$; (B) $\phi = 0.195$.

Table 1. Properties of a TPM Silica Dispersion in MMA^a

ϕ	time (h)	λ_{\max} (nm)	bandwidth (nm)	d_{111}^b (nm)
0.227 ^c	8	532	3.6	188.1
0.195 ^d	72	552	3.4	195.2

^a ϕ = volume fraction of particles; λ_{\max} = diffracted wavelength maximum; time = time between filling of the cells and measurement of the spectra; bandwidth at half-maximum intensity. ^b Calculated from eq 1 using refractive indexes of the TPM silica particles 1.449¹⁴ and of the MMA 1.4142. ^c Number average diameter 153 nm. ^d Number average diameter 152 nm.

entire cell fills with crystallites, and the sample turns from cloudy to iridescent. The crystals in most of the cell are at extinction, indicating fcc(111) planes normal to the light path, and they appear purple when the cell is rotated 40–55° to the incident plane polarized light. After 4–7 days only crystals at the sample edges are still birefringent with light normal to the sample plane.

Figure 1 shows visible spectra of the colloidal dispersions containing ordered arrays of crystals. Neither the silica particles nor the MMA absorbs in the visible range. The sharp peaks are due to Bragg diffraction of light by the colloidal crystals. Table 1 reports the compositions and spectral data. The spectrophotometer detects light transmitted through an ~8-mm circular cross section of the cell, which contains approximately 10² crystallites. The spectra are reproducible as long as the light focuses normal to the fcc(111) planes, which are parallel to the film plane. We calculated theoretically the d spacing for fcc(111) crystals from volume fraction ($\phi = 0.195$), particle diameter, and lattice parameter¹³ and found $d = 193.6$ nm, close to that calculated from the experimental λ_{\max} ($=\lambda_{\text{corr}}$) via eq 1. The λ_{\max} in MMA shifts to longer wavelength as the volume percent of the particles decreases, indicating the wavelength dependence on lattice spacing. Two different batches of TPM-silica in MMA showed similar crystalline behavior. The bandwidths of diffracted light from 264- μm cells are 3.4–3.6 nm. A bandwidth of 3.1 nm was calculated by the method of eq 15 of Spry and Kosan,¹⁵ in excellent agreement with our observations even though more planes contribute to diffraction in the silica-MMA dispersions than in dispersions of polystyrene latexes in water. A higher degree of order of the crystallites, a smaller difference between the refractive indexes of the particles and the monomer, and smaller particle diameters all narrow the bandwidth of the diffracted light from the dispersions.^{11,12} Using 332-nm TPM silica particles in MMA, we observed a 33-nm

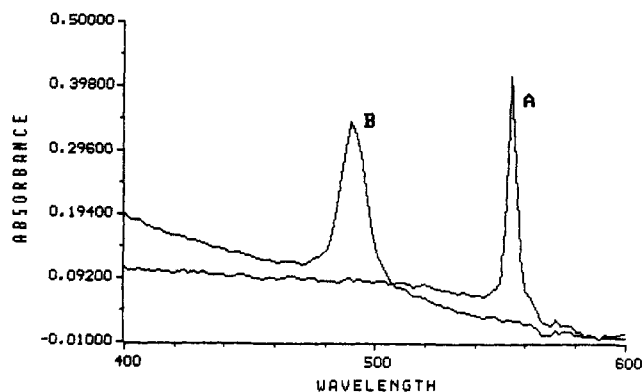


Figure 2. Visible spectra of TPM silica (A) in MMA before polymerization and (B) after polymerization.

Table 2. Properties of a PMMA Composite and a MMA Dispersion^a

	ϕ	n_s^b	λ_{\max} (nm)	bandwidth (nm)	
				obsd	calcd ^c
MMA	0.195	1.4210	554	4.0	3.1
PMMA	0.235 ^d	1.4819	490	13.6	3.7

^a Same sample as line 2 of Table 1, polymerized after standing 4 more days, during which the λ_{\max} and the bandwidth both increased slightly. ^b Calculated from eq 2 using $n = 1.492$ for PMMA. ^c Using eq 15 from ref 15. ^d Calculated assuming a 21% decrease in volume of the matrix during polymerization.

bandwidth of diffracted light, which verifies the effect of particle size. The degree of ordering of the crystallites is also influenced by the cell thickness:^{11,16} the thinner the sample, the greater the order of crystallites. We observe no significant differences of the bandwidths of diffracted peaks between dispersions in 132- and 264- μm cells.

PMMA Composites. When the dispersions turned from cloudy to iridescent, indicating formation of colloidal crystals throughout the sample, we polymerized the dispersions containing 1 wt % photoinitiator. The TPM groups on the silica copolymerize with MMA as shown in Scheme 1. The amount of the photoinitiator and its extinction coefficient of 274 M⁻¹ cm⁻¹ at $\lambda_{\max} = 336$ nm indicate there should be uniform irradiation throughout the 264- μm glass cell. The cell must be kept horizontal during crystal growth and polymerization to prevent sedimentation of the particles. During photopolymerization of horizontal films the order of the lattice planes of the crystals was slightly disturbed according to the increased diffraction bandwidth. Figure 2 shows the diffraction bands of the colloidal crystals before and after polymerization, and Table 2 reports the data. The composite has a rejection peak at 490 nm with a bandwidth of 13.6 nm.

The orthoscopic polarizing microscopic images of the polymerized films show few colored crystallites and many at extinction, similar to the dispersions. When the composite films were rotated 40–55° to the incident light, mostly purple and a few green crystals appeared throughout the film. This indicates that the order of the crystallites in the monomer is maintained and trapped in the solid matrix.

Light microscopy and freeze fracture electron microscopy have been used previously to visualize directly the

(15) Spry, R. J.; Kosan, D. J. *Appl. Spectrosc.* 1986, 40, 782.

(16) Van Winkle, D. H.; Murray, C. A. *Phys. Rev. A* 1986, 34, 562.

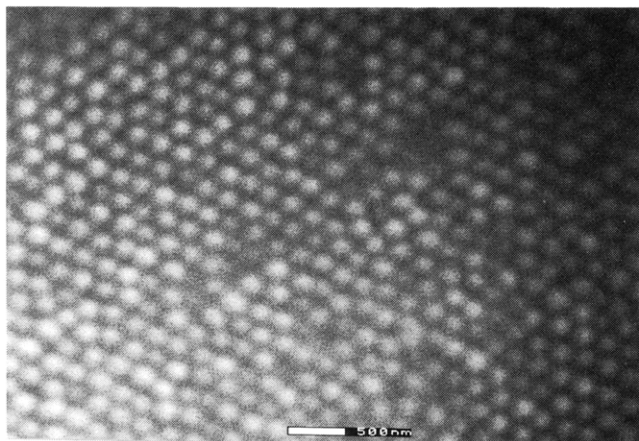


Figure 3. SEM photograph of the polymerized film of Table 2. The film was coated with Ag-Pd, and the micrograph was taken at 15 kV and 20 000 times magnification.

ordered array of polystyrene particle dispersions.¹⁷⁻¹⁹ Figure 3 shows a SEM of the surface layer of a composite film. The SEM reveals that the fcc d_{111} plane of silica

(17) Kose, A.; Ozaki, M.; Takano, K.; Kobayashi, Y.; Hachisu, S. *J. Colloid Interface Sci.* **1973**, *44*, 330.

(18) Okubo, T. *J. Chem. Phys.* **1987**, *86*, 2394.

(19) Cohen, J. A.; Scales, D. J.; Ou-Yang, H. D.; Chaikin, P. M. *J. Colloid Interface Sci.* **1993**, *156*, 137.

particles parallel to the surface in the liquid dispersion is retained in the solid matrix. The average center-to-center distance between neighboring particles measured from the micrograph is 233.8 nm, and the average surface-to-surface distance is 82 nm, indicating that the order is due to the long-range repulsions rather than hard-sphere packing.

Though the Bragg diffraction of visible light from the glassy film is evident from the visible spectrum and from the polarizing microscope, there are marked differences between the colloidal dispersion and the composite. According to eq 1, an increased refractive index will increase the diffracted wavelength, and decreased d spacing will decrease the diffracted wavelength. A blue shift in the rejection wavelength of the composite material indicates that the colloidal crystals are compressed during photopolymerization. The expected 21% decrease in volume of MMA by polymerization accounts for a 6.8% decrease in d spacing, compared with an observed 14.7% decrease of d , which must be due to an increase of particle number within the crystalline regions. The greater bandwidth of the diffraction peak of the composite film could be due to lower crystalline order of the particles in the polymer film than in the dispersion.

Acknowledgment. This work was supported by National Science Foundation Grant DMR-9024858. We thank Bruce J. Ackerson for helpful discussion.